Hindawi Publishing Corporation
BioMed Research International
Volume 2013, Article ID 902427, 12 pages
http://dx.doi.org/10.1155/2013/902427

Research Article

Effect of Boron Addition on the Thermal, Degradation, and Cytocompatibility Properties of Phosphate-Based Glasses

Nusrat Sharmin,[1] Muhammad S. Hasan,[1] Andrew J. Parsons,[1] David Furniss,[2] Colin A. Scotchford,[1] Ifty Ahmed,[1] and Chris D. Rudd[1]

[1] *Division of Materials, Mechanics and Structures, Faculty of Engineering, University of Nottingham, Nottingham NG7 2RD, UK*
[2] *Division of Electrical Systems and Optics, Faculty of Engineering, University of Nottingham, Nottingham NG7 2RD, UK*

Correspondence should be addressed to Ifty Ahmed; ifty.ahmed@nottingham.ac.uk

Received 5 April 2013; Revised 1 July 2013; Accepted 2 July 2013

Academic Editor: Stanley J. Stachelek

In this study eight different phosphate-based glass compositions were prepared by melt-quenching: four in the $(P_2O_5)_{45}$-$(CaO)_{16}$-$(Na_2O)_{15-x}$-$(MgO)_{24}$-$(B_2O_3)_x$ system and four in the system $(P_2O_5)_{50}$-$(CaO)_{16}$-$(Na_2O)_{10-x}$-$(MgO)_{24}$-$(B_2O_3)_x$, where $x = 0, 1, 5$ and 10 mol%. The effect of B_2O_3 addition on the thermal properties, density, molar volume, dissolution rates, and cytocompatibility were studied for both glass systems. Addition of B_2O_3 increased the glass transition (T_g), crystallisation (T_c), melting (T_m), Liquidus (T_L) and dilatometric softening (T_d) temperature and molar volume (V_m). The thermal expansion coefficient (α) and density (ρ) were seen to decrease. An assessment of the thermal stability of the glasses was made in terms of their processing window (crystallisation onset, $T_{c,ons}$ minus glass transition temperature, T_g), and an increase in the processing window was observed with increasing B_2O_3 content. Degradation studies of the glasses revealed that the rates decreased with increasing B_2O_3 content and a decrease in degradation rates was also observed as the P_2O_5 content reduced from 50 to 45 mol%. MG63 osteoblast-like cells cultured in direct contact with the glass samples for 14 days revealed comparative data to the positive control for the cell metabolic activity, proliferation, ALP activity, and morphology for glasses containing up to 5 mol% of B_2O_3.

1. Introduction

There is a continually growing interest in the use of glasses for varying biomedical applications. Bioactive glasses are a group of surface reactive glasses which can initiate a range of biological responses by releasing ions into the local environment [1]. The first bioactive glass reported was bioglass discovered by Professor Larry Hench in 1969 [2]. Professor Hench and his colleagues investigated a range of silicate-based compositions, and the composition formed consisted of 45% SiO_2, 24.5% Na_2O, 24.5% CaO, and 6% P_2O_5 (expressed as wt%) also known as 45S5 [3]. An alternate system of glasses for biomedical applications is totally silica free phosphate-based glasses (PBGs). These PBGs have the property of being completely soluble in aqueous medium, and their degradation rate can easily be altered via addition of different modifier oxides. These unique physical and chemical properties of PBGs have attracted huge interest in their use within the field of biomaterials and tissue engineering [4–6].

The structure of PBGs is composed of an inorganic phosphate network in which PO_4^{3-} tetrahedral units are the main building blocks. The tetrahedra can be described in terms of Q^n terminology, where n represents the number of bridging oxygens (BOs) per PO_4^{3-} tetrahedron. The prevalence of any particular Q species is dependent on the oxygen-to-phosphorous (O/P) ratio in the glass which is determined by the addition of different metal oxides (MeO) [7]. As the ratio MeO/P_2O_5 increases from 0 to 3, the phosphate structural groups pass from Q^3 to Q^0 [8].

Various formulations of PBGs have been studied extensively for their biocompatibility. Different studies showed that the biocompatibility of these glasses was affected strongly by their degradation rate and associated ion release [6]. Therefore, the biocompatibility of PBGs is expected to be affected by the addition of different metal oxides, which are known to alter the chemical durability of the glasses. Ahmed et al. investigated four invert glasses in the system of P_2O_5-CaO-MgO-Na_2O with fixed phosphate and calcium contents

at 40 and 25 mol%, and Na_2O was replaced with 10–30 mol% MgO [9]. They found that the degradation rates for these glasses decreased with increasing MgO and suggested that the degradation profiles and cytocompatibility properties of these glasses were suitable for bone repair applications.

Cell culture studies of the glasses in the system P_2O_5-CaO-MgO-Na_2O-Fe_2O_3 using MG63 cells showed that these glasses possessed good cellular response in terms of cell viability, proliferation, and differentiation [10]. Therefore, PBGs can be synthesised with different network modifiers capable of inducing different biological functions with enhanced biocompatibility.

A wide variety of glass network structures can be expected from the combination of two glass network formers such as P_2O_5 and B_2O_3 [11, 12]. NMR analysis of borophosphate glasses revealed that the addition of boron increased the chain lengths (Q^2 species) in the glass structure [13]. Several studies also showed that addition of B_2O_3 to the phosphate network improved the chemical durability and thermal properties of the glasses [14–17]. The addition of B_2O_3 was also known to improve the thermal stability of these glasses by suppressing their tendency to crystallise [16, 18], which is a common problem associated with the drawing of phosphate glass fibres as they have a tendency towards crystallisation at the working process temperature [19], particularly with Q^0 and Q^1 dominated structures. Therefore, it was hypothesised that addition of boron may overcome this problem and make the fibre drawing process easier especially for glasses with phosphate contents lower than 50 mol%.

Recently, it has been shown that some borate glasses can accelerate the formation of a hydroxyapatite layer and bond to bone in a manner which is comparable to 45S5 glasses [13, 20]. Saranti et al. reported that the bioactivity of pure calcium phosphate glasses was favoured by the presence of boron in the glass network due to the ability of boron to change coordination and attach hydroxyl groups at the surface of the glasses [13]. Nielson highlighted that boron played an important role in bone growing than its maintenance [21]. Boron has been speculated to have stimulated hormones, thus mimicking the effects of oestrogen, producing an oestrogen replacement. Currently, oestrogen treatment is still one of the most effective methods of preventing postmenopausal bone loss [21]. Thus, the delivery of boron via the degradation of boron containing degradable PBGs could be of special interest in biomedical applications.

The initial aim of this study was to investigate the effect of B_2O_3 addition on the thermal, degradation, and cytocompatibility properties of PBG glasses in the system P_2O_5-CaO-MgO-Na_2O with phosphate contents fixed at 45 and 50 mol%. The final aim was to produce continuous soluble phosphate-based glass fibres (PGF), which could be used as reinforcement for different resorbable polymers (such as Ploylactic acid) to make composites for different biomedical applications. Dissolution studies of the glasses were conducted in phosphate buffer saline (PBS) solution, and the MG63 osteosarcoma cell line was used for the cytocompatibility studies. Furthermore, the effect of B_2O_3 addition on the density and molar volume of the glass system was also evaluated.

2. Materials and Methodology

2.1. Glass Preparation. Eight different glass compositions were prepared using sodium dihydrogen phosphate (NaH_2PO_4), calcium hydrogen phosphate ($CaHPO_4$), magnesium hydrogen phosphate trihydrate ($MgHPO_4{\cdot}3H_2O$), boron oxide (B_2O_3), and phosphorous pentoxide (P_2O_5) (Sigma Aldrich, UK) as starting materials. The precursors were mixed together and transferred to a 100 mL volume Pt/5% Au crucible (Birmingham Metal Company, UK) which was then placed in a furnace (preheated to 350°C) for half an hour for the removal of H_2O. The salt mixtures were then melted in a furnace at 1150°C for 1.5 hours, depending on the glass composition as shown in Table 1. Molten glass was poured onto a steel plate, left to cool, and then ground into powder using a pestle and mortar. Having obtained the T_g of the glass via DSC (see the thermal analysis section), it was then remelted and casted as 9 mm diameter rods by being poured into a graphite mould preheated at different temperatures (as stated in Table 1). The mould was then held at the casting temperature (see Table 1) for an hour and then allowed to cool to room temperature to remove any residual stress.

2.2. Thermal Analysis. Glass pieces of the various compositions were ground to fine powder using a pestle and mortar. The glass transition temperature (T_g) of the glasses was determined using differential scanning calorimeter (DSC, TA Instruments Q10, UK). A sample of each glass composition was heated from room temperature to 520°C at a rate of 20°C min^{-1} in flowing argon gas. The T_g was extrapolated from the onset of change in the endothermic reaction of the heat flow [22].

To determine the onset of crystallisation, peak crystallisation, and melting and liquidus temperatures, an alternate DSC instrument (TA Instruments SDT Q600, UK) was used. Samples were heated from room temperature to a value of T_g + 20°C at a rate of 20°C min^{-1}, held there isothermally for 15 min, and then cooled down at a rate of 10°C min^{-1} to 40°C before ramping up again to 1100°C at a rate of 20°C min^{-1} under flowing argon gas. The samples were subjected to the programmed heating cycle to introduce a known thermal history. A blank run was carried out to determine the baseline which was then subtracted from the traces obtained. The T_g was determined from the second ramping cycle in the same process discussed above. The first deviation of the DSC curve from the baseline above T_g before crystallisation peak was taken as the onset of crystallisation temperature. The thermal stability of the glasses was measured in terms of the processing window by taking the temperature interval between T_g and the onset of crystallisation temperature ($T_{c,ons}$) as shown in the following:

$$\text{processing window} = T_{c,ons} - T_g \quad (1)$$

2.3. Thermomechanical Analysis. The thermal expansion coefficient (α) and dilatometric softening temperature (T_d) were measured using a thermomechanical analyser TMA (TA Instruments TMA Q400, UK). Three samples from each composition of an average 7 mm height and 9 mm diameter

Table 1: Glass codes and drying, melting, and casting temperatures used throughout the study.

Glass code	P_2O_5 content (mol%)	CaO content (mol%)	Na_2O content (mol%)	MgO content (mol%)	B_2O_3 content (mol%)	Drying temp/time (°C/h)	Melting temp/time (°C/h)	Casting temp/time (°C/h)
P45B0	45	16	15	24	—	350/1	1150/1.5	450/1
P45B1	45	16	14	24	1	350/1	1150/1.5	456/1
P45B5	45	16	10	24	5	350/1	1150/1.5	484/1
P45B10	45	16	5	24	10	350/1	1150/1.5	510/1
P50B0	50	16	10	24	—	350/1	1150/1.5	460/1
P50B1	50	16	9	24	1	350/1	1150/1.5	474/1
P50B5	50	16	5	24	5	350/1	1150/1.5	492/1
P50B10	50	16	—	24	10	350/1	1150/1.5	560/1

were heated at a rate of 5°C min^{-1} with an applied load of 50 mN. The measured thermal expansion coefficient (α) was taken as an average between 50°C and 250°C. The T_d was taken as the midway point (on the ordinate) between the abrupt increase in expansion and the onset of contraction.

2.4. Helium Pycnometry. The density of the glasses was determined by using a MicromeriticsAccuPyc 1330 helium pycnometer (Norcross, GA, USA). The equipment was calibrated using a standard calibration ball (3.18551 cm^3) with errors of ±0.05%. Bubble-free bulk glass samples, with an average weight of approximately 6.5 g, were used for the density measurements, and the process was repeated three times. For each composition the molar volume (V_m) was also calculated using the following equation:

$$V_m = \frac{\sum (x_i \cdot M_i)}{\rho}, \quad (2)$$

where ρ is the density, x_i is the molar fraction of i component, and M_i is the molecular weight for component i.

2.5. Powder X-Ray Diffraction Analysis. The amorphous state of all the glass compositions was confirmed using X-ray diffraction spectra obtained from a Bruker D500 X-ray diffractometer at room temperature with Ni-filtered CuKα-radiation (λ = 0.15418 nm), operated at 40 kV and 40 mA. The angular range 2θ for each scan was from 15° to 100° with a step size of 0.02° and a step time of 0.5 s.

2.6. Dissolution Studies. Glass rods of 9 mm diameter were cut into 5 mm thick discs using a low speed saw (South Bay Technologies, CA, USA) equipped with a diamond blade (Buehler, Coventry, UK). Ethanol (Fisher Chemicals, UK) was used as a lubricating fluid. The surface area of the glass discs was measured using a micrometer, and the discs were placed in glass vials containing 30 mL of phosphate buffer solution (PBS). These vials were then placed into an incubator at 37°C. At various time points, the discs were taken out from the vials, excess moisture was removed by blotting the samples dry with tissue, and the area and mass were measured. The dissolution study was carried out for 60 days, and the PBS solution was changed at each time point. During the first week, the mass loss and surface area were measured every day. For the following weeks, the measurements were taken twice a week. Thus the time points were day 1, 2, 3, 4, 7, 10, 14, 16, 20, 23, 27, 30, 34, 36, 44, 47, 50, 54, and 60. The rate of mass loss (%) was calculated according to the following equation:

$$\text{mass loss (\%)} = \frac{M_0 - M_t}{M_0}, \quad (3)$$

where M_0 is the initial mass (g) and M_t is the mass at time t. The mass loss per area data was plotted as weight loss per unit area against time. The slope of this graph gave the dissolution rate in terms of g cm^{-2} h^{-1}.

2.7. Cell Culture. MG63 cells (human osteosarcoma), obtained from the European Collection of Cell Cultures (ECACC), were cultured in complete Dulbecco's Modified Eagle Medium (CDMEM) consisting of DMEM supplemented with 10% foetal calf serum (FCS), 2% HEPES buffer, 2% penicillin/streptomycin, 1% glutamine, 1% nonessential amino acids (Gibco Invitrogen, UK), and 0.85 mM of ascorbic acid (Sigma Aldrich, UK). Cells were cultured in 75 cm^3 flasks (Falcon, Becton, Dickinson and Company, UK) at 37°C in a humidified atmosphere with 5% CO_2. The glass discs were sterilised using dry heat at 190°C for 15 minutes and washed three times with sterilised PBS prior to cell culture. Tissue culture plastic (TCP) was used as an internal control for cell growth. Cells were seeded onto the disc sample surfaces at 40,000 cells/cm^2 concentration and incubated at 37°C in a humidified atmosphere with 5% CO_2.

2.8. Cell Viability/Metabolic Activity. At designated time points, culture medium was removed from the wells, and the samples were washed three times with warm PBS. Alamar Blue solution (1 : 9 Alamar Blue: warm hanks balanced salt solution (HBSS)) (1 mL) was added to each well and incubated for 90 minutes. From each well, 100 μL aliquots were transferred to a 96 well-plate in triplicate, and fluorescence was measured at 530 nm excitation and 590 nm emission using FLx800 microplate reader (BioTek Instruments Inc.).

2.9. Proliferation. At designated time points cell culture media was removed, and the samples were washed three times

with warm PBS prior to addition of 1 ml deionised water to each well. Cells were lysed using a freeze/thaw technique three times.

100 μL aliquots of cell lysate were transferred to a 96-well plate. DNA standards were prepared using calf thymus DNA (Sigma, UK) and TNE buffer (10 mMTris, 2 M NaCl, and 1 mM EDTA in deionised water, adjusted to pH 7.4) as a diluent. One hundred microlitres of Hoechst stain 33258 was added to each well (1 mg of bis-benzimide 33258 in deionised water, further diluted to 1 : 50 in TNE buffer), and the plate was agitated. Fluorescence was measured at 360 nm excitation and 460 nm emission using a FLx800 microplatefluorimeter (BioTek Instruments Inc.). DNA concentrations were derived from a standard curve of known DNA concentrations generated by the software (KCjunior).

2.10. Alkaline Phosphatase Activity. Alkaline phosphatase activity was measured using the Granutest 25 alkaline phosphatase assay (Randox, UK). A 50 μL aliquot of cell lysate (as prepared for DNA quantification assay) was added to a 96-well plate along with 50 mL of the alkaline phosphatase substrate (p-nitrophenyl phosphate in diethanolamine HCI buffer, pH 9.8) and shaken gently, and the absorbance was measured at wavelengths of 405 and 620 nm using a ELx800 microplate colorimeter (BioTek Instruments Inc).

2.11. Morphology. Samples were washed with warm PBS at 37°C and fixed in 3% glutaraldehyde in 0.1 M nacacodylate buffer for 30 minutes. After 30 minutes, the fixative was replaced by 7% sucrose solution. Fixed samples were then washed twice in 0.1 M Na-cacodylate buffer and postfixed in 1% osmium tetroxide in PBS for 45 minutes in a fume cupboard. Samples were dehydrated through a graded ethanol series (20, 30, 40, 50, 60, 70, 80, 90, 96, and 100% in water) for approximately 5 minutes each and then dried via hexamethyldisilazane (HMDS) before being sputter-coated in platinum and viewed with a Philips XL30 scanning electron microscope operated at 10 kV.

2.12. Statistical Analyses. Average values and standard deviation were computed, and statistical analysis was performed using the Prism software package (version 3.02, GraphPad Software, San Diego, CA, USA, http://www.graphpad.com). Two-way analysis of variance (ANOVA) was calculated with the bonferroni post-test to compare the significance of change in one factor with time. The error bars presented represent standard deviation with $n = 3$.

3. Results

3.1. Powder X-Ray Diffraction Analysis. XRD traces for the glass samples are presented in Figure 1 below, where a single broad peak between 20° and 40° was observed for each composition. The absence of any sharp crystalline peaks confirmed that all the glasses produced were amorphous.

3.2. Thermal Analysis. Figure 2 shows the effect of increasing B_2O_3 content on T_g values for glasses in the $P_{45}Ca_{16}Mg_{24}Na_{15-x}B_x$ and $P_{50}Ca_{16}Mg_{24}Na_{(10-x)}B_x$ systems

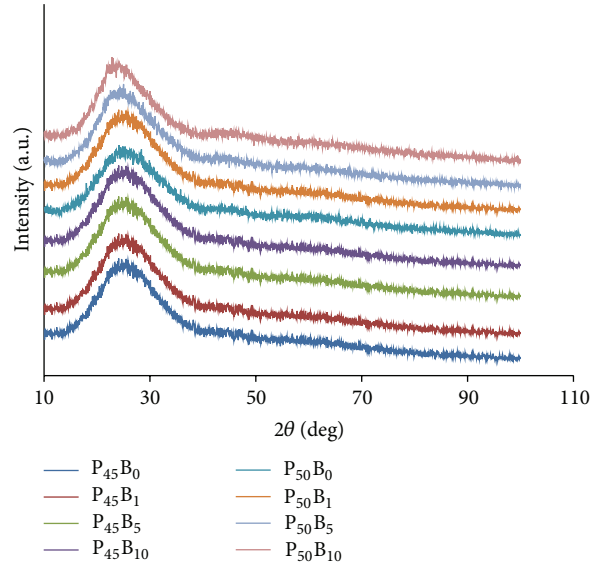

Figure 1: Powder X-ray diffraction pattern for glasses in the system of $P_{45}Ca_{16}Mg_{24}Na_{(15-x)}B_x$ and $P_{50}Ca_{16}Mg_{24}Na_{(10-x)}B_x$.

(where $x = 0, 1, 5$, or 10). The T_g values increased with increasing B_2O_3 content. An increase in T_g was also observed with increasing P_2O_5 content from 45 to 50 mol%. An increase of 50°C in T_g values was observed with increasing P_2O_5 content from 45 to 50 mol% for the 10 mol% B_2O_3 containing glasses, whilst, for the other glass formulations investigated, a difference of ≈10°C in T_g values was observed with increasing P_2O_5. For glasses containing 45 mol% P_2O_5 (P45), the T_g values increased from 440 to 500°C as Na_2O was replaced by B_2O_3. For glasses with fixed 50 mol% P_2O_5 (P50), an increase from 452 to 552°C was observed. Thermal scans for the series of glasses investigated in the $P_{45}Ca_{16}Mg_{24}Na_{(15-x)}B_x$ and $P_{50}Ca_{16}Mg_{24}Na_{(10-x)}B_x$ systems are shown in Figures 3(a) and 3(b), respectively. The corresponding onset of crystallisation ($T_{c,ons}$), crystallisation peak (T_c), melting peak (T_m), and liquidus (T_L) temperature have been labelled on the thermal traces obtained.

The onset of crystallisation was found to increase with increasing boron content in each glass system. The thermal scans of all the compositions exhibited two crystallisation (T_{c1} and T_{c2}) and melting peaks (T_{m1} and T_{m2}); in addition, the intensity of the crystallisation peaks decreased and became less defined with increasing boron content. A summary of $T_{c,ons}$, T_c, T_m, and T_L is given in Table 2.

The values for the processing window ($T_{c,ons} - T_g$), which is also an indication of the thermal stability for glasses, are presented in Figure 4. The values for the processing window were seen to increase with increasing B_2O_3 content for both the P45 and P50 glasses. With 5 mol% B_2O_3 addition, the processing window increased from 86°C to 110°C with increasing P_2O_5 content from 45 to 50 mol%. The processing window for P45B0 and P50B0 glasses was 74°C and 87°C, respectively. Whereas, the processing window increased to 112°C and 123°C for P45B10 and P50B10 glasses, respectively.

Table 2: The thermal characteristics (T_x, T_c, T_m, T_L) for $P_{45}Ca_{16}Mg_{24}Na_{(15-x)}B_x$ and $P_{50}Ca_{16}Mg_{24}Na_{(10-x)}B_x$ (x = 0–10) glass systems.

Glass code	$T_{c,ons}$/°C	T_c/°C	T_m/°C	T_L/°C
P45B0	512.2 ± 0.5	535.4 ± 0.7 609.3 ± 0.4	809.7 ± 0.1 838.0 ± 0.3	864.3 ± 3.0
P45B1	513.2 ± 1.3	539.3 ± 1.5 609.4 ± 0.3	812.3 ± 0.1 838.3 ± 0.3	864.1 ± 0.1
P45B5	561.6 ± 1.7	559.7 ± 0.8 759.8 ± 0.8	821.9 ± 0.1 892.4 ± 0.3	972.0 ± 0.3
P45B10	615.2 ± 3.5	660.1 ± 0.3 865.1 ± 1.0	932.7 ± 0.3 995.1 ± 1.0	1011.4 ± 0.4
P50B0	538.2 ± 1.7	614.31 ± 1.7	832.0 ± 0.1 887.4 ± 0.3	903.10 ± 0.3
P50B1	543.0 ± 0.3	573.3 ± 0.3 654.8 ± 1.0	827.9 ± 2.5 880.6 ± 0.0	901.5 ± 1.0
P50B5	589.9 ± 0.7	637.2 ± 1.0 758.54 ± 4.8	829.1 ± 0.0 970.51 ± 6.6	1031.5 ± 0.6
P50B10	669.1 ± 1.5	745.8 ± 0.8 942.8 ± 0.8	1029.4 ± 0.3 1059.7 ± 0.4	1091.9 ± 0.6

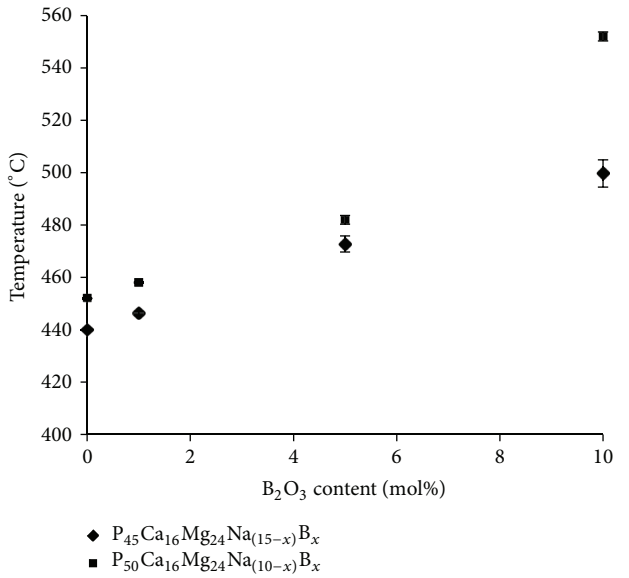

Figure 2: Glass transition temperature (T_g) as a function of the B_2O_3 content (mol%) in the system of $P_{45}Ca_{16}Mg_{24}Na_{15-x}B_x$ and $P_{50}Ca_{16}Mg_{24}Na_{(10-x)}B_x$ (x = 0–10) glass system.

3.3. Thermal Expansion Coefficient and Dilatometric Softening Temperature Measurements. Dilatometric measurements provided the values for thermal expansion coefficient α (measured between 50°C and 250°C) and the dilatometric softening temperature (T_d) (see Figure 5). The values for α were seen to decrease with increasing B_2O_3 content from 14 $\times 10^{-6}$°C to 11 $\times 10^{-6}$°C and from 12 $\times 10^{-6}$°C to 8 $\times 10^{-6}$°C for P45 and P50 glasses, respectively. The dilatometric softening temperatures increased from 452°C to 526°C and from 472°C to 586°C with 10 mol% B_2O_3 addition to the P45 and P50 glasses, respectively.

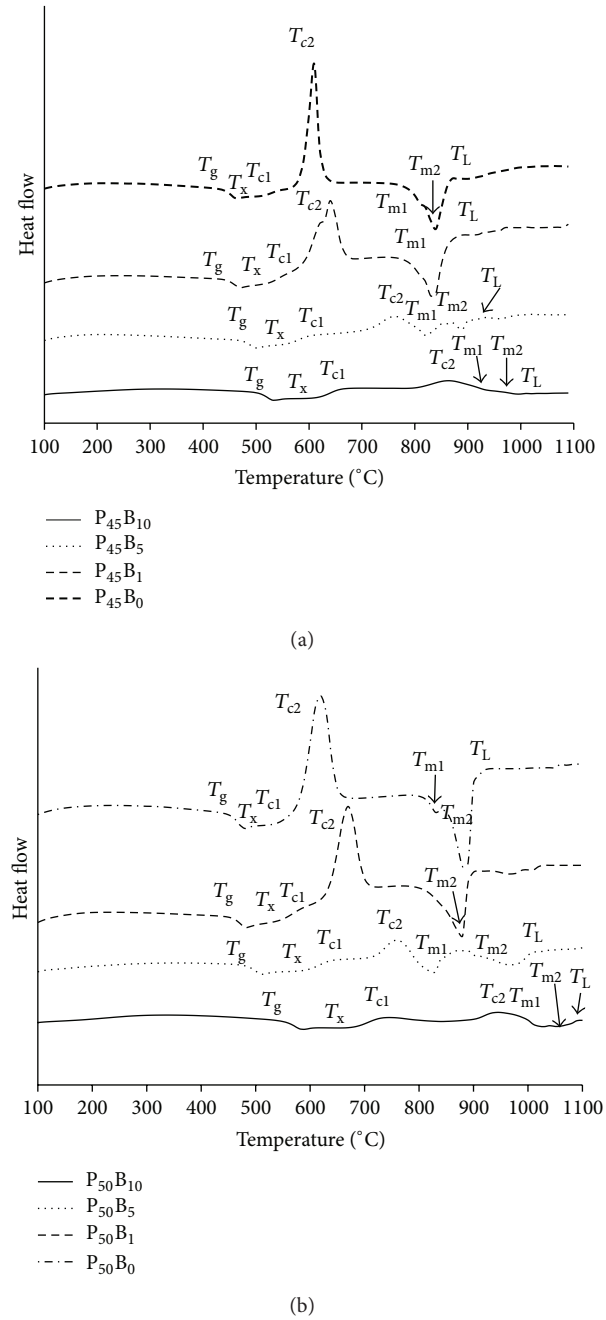

Figure 3: Thermal scans for the glass series in the (a) $P_{45}Ca_{16}Mg_{24}Na_{(15-x)}B_x$ and (b) $P_{50}Ca_{16}Mg_{24}Na_{(10-x)}B_x$ (x = 0–10 mol%) glass system.

3.4. Density and Molar Volume Measurements. Figure 6 shows the variation in density (ρ) and molar volume (V_m) with increasing B_2O_3 content of the glasses. The density was seen to decrease from 2.65 to 2.62 $\times 10^3$ kg m^{-3} for P45 glasses and from 2.59 to 2.53 $\times 10^3$ kg m^{-3} for P50 glasses with increasing boron content. Consequently, for the P45 glasses the molar volume increased from 34.7 to 35.4 $\times 10^{-6}$ m^3 mol^{-1}, and for the P50 glasses an increase from 37.0 to 38.14 $\times 10^{-6}$ m^3 mol^{-1} was observed with increasing boron content.

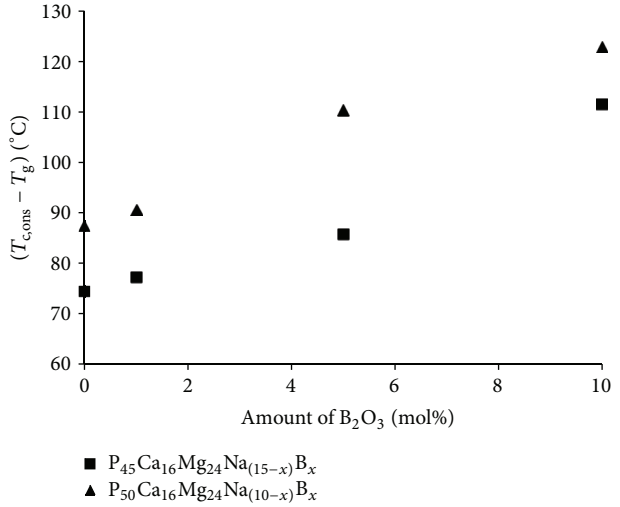

Figure 4: Processing window (crystallisation onset, $T_{c,ons}$ minus glass transition temperature, T_g) as a function of B_2O_3 content (0–10 mol%).

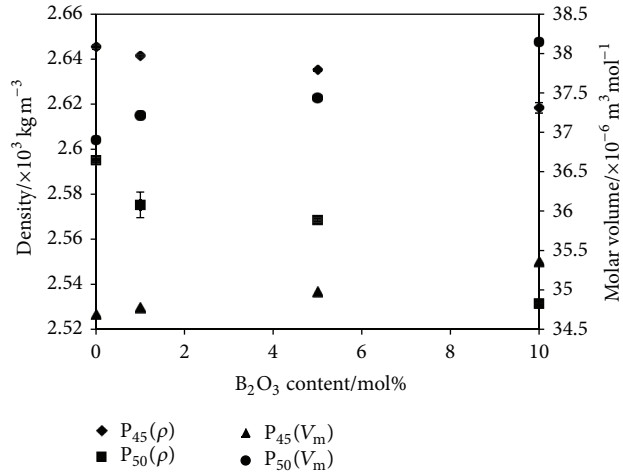

Figure 6: Plot of density (ρ) and molar volume (V_m) of the glasses in the system of $P_{45}Ca_{16}Mg_{24}Na_{(15-x)}B_x$ and $P_{50}Ca_{16}Mg_{24}Na_{(10-x)}B_x$ (x = 0–10) as a function of B_2O_3 content (0–10 mol%).

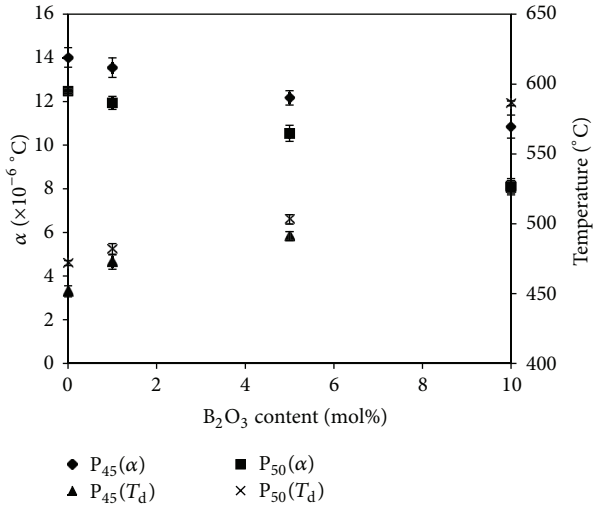

Figure 5: Thermal expansion coefficient (α) and dilatometric softening temperature (T_d) of the glasses in the system of $P_{45}Ca_{16}Mg_{24}Na_{(15-x)}B_x$ and $P_{50}Ca_{16}Mg_{24}Na_{(10-x)}B_x$($x$ = 0–10) as a function of B_2O_3 content (mol%). The values of α is measured in the range between 50 and 250°C.

3.5. Glass Solubility. Figures 7(a) and 7(b) show the mass loss (%) of the glasses as a function of immersion time in phosphate buffer solution at 37°C for P45 and P50 glasses, respectively. No significant difference ($P < 0.05$) in mass loss was seen for glasses containing 0 and 1 mol% B_2O_3. However, with further increase in B_2O_3 content (5–10 mol%), the mass loss decreased. At 10% B_2O_3 addition, the total mass loss observed over the full duration of the 60-day study was seen to decrease from 3.01 to 1.30% for P45 glasses, and for P50 glasses a reduction from 3.24 to 1.40% was observed.

Figure 8 is a 3D representation of the dissolution rates obtained for the glasses investigated. With addition of B_2O_3 at the expense of Na_2O, the dissolution rate decreased. After 60 days, the dissolution rate for the P45B0 and P50B0 glasses was 1.85×10^{-4} and 1.89×10^{-4} g cm^{-1} day^{-1}, whilst the dissolution rate decreased to 8.57×10^{-5} and 9.85×10^{-5} g cm^{-1} day^{-1} for P45B10 and P50B10 glasses, respectively. A decrease in dissolution rate was also observed with decreasing P_2O_5 content from 50 to 45 mol%.

3.6. Cytocompatibility Studies

3.6.1. Cell Viability/Metabolic Activity. The Alamar Blue assay was used to determine the effect of boron addition on the metabolic activity of osteoblast-like cells (MG63). The cells were cultured for 14 days, and the time points were day 1, 3, 7, and 14 (Figure 9).

Metabolic activity was seen to increase throughout the 14-day culture period. The TCP control demonstrated faster metabolic activity compared to other samples at early time points (up to 7 days), which was statistically significant ($P < 0.001$). Cell metabolic activity on P50 glasses, especially P50B0 and P50B1, was seen to be significantly lower ($P < 0.01$) on the 7th day compared to the P45 glasses. However, at the latter time points all glass samples demonstrated similar levels of metabolic activity to the TCP control.

3.6.2. Alkaline Phosphatase Activity. The effect of boron addition to PBGs on the osteoblast-like phenotype was analysed by measuring the alkaline phosphatase activity of osteosarcoma cells (see Figure 10). Data was normalised with the corresponding DNA concentration at each time point.

For all samples, including the TCP (internal control), the ALP activity was not detectable up to 3 days. However, after 7 days of culture, detectable amounts of ALP activity were observed on all samples, with notably overall higher ALP activity on P45 formulations. The ALP activity of cells cultured on P45 PBG containing 0–10% boron was significantly higher ($P < 0.05$) than the other glass samples investigated with the exception of glass code P50B5. After 14

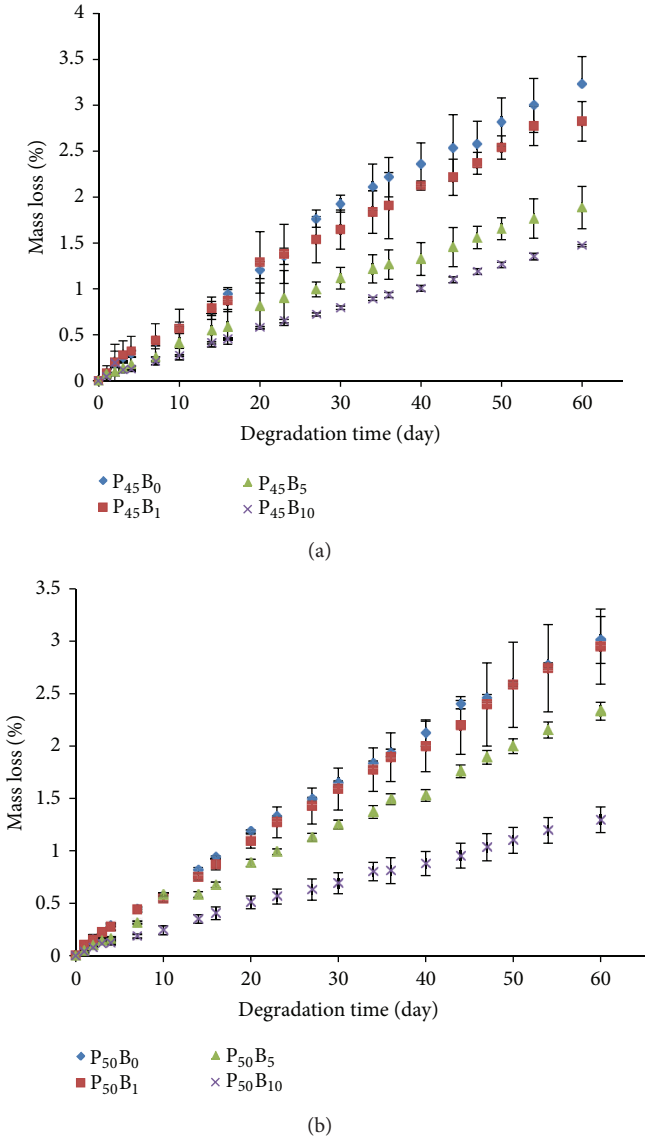

FIGURE 7: Plot of mass loss (%) of the glasses in the system of (a) $P_{45}Ca_{16}Mg_{24}Na_{(15-x)}B_x$ and (b) $P_{50}Ca_{16}Mg_{24}Na_{(10-x)}B_x$ (x = 0–10) in PBS at 37°C for 60 days.

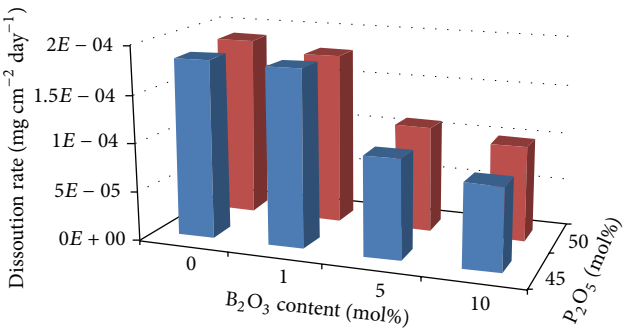

FIGURE 8: 3D graph of dissolution rate values obtained for glasses fixed with 45 and 50 mol%.

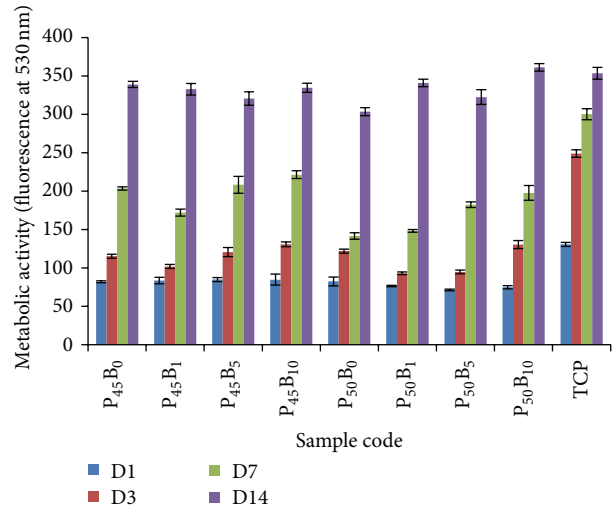

FIGURE 9: Metabolic activity of MG63 cells, as measured by the Alamar Blue assay, cultured on PBGs. The time points are day 1, 3, 7, and 14. Error bars represent the standard deviation where $n = 6$.

days, no significant difference ($P > 0.05$) was observed between P45 and P50 containing 0–5% boron. However, both P45 and P50 glasses containing 10% boron appeared to have a less influence on ALP compared to 5 mol% B_2O_3 doped glasses; nonetheless, they were still comparable to the TCP control ($P > 0.05$).

3.6.3. Morphology. The morphology of the cells cultured on phosphate glass discs was visualised using SEM (see Figure 11). A representative image of MG63 osteosarcoma cells cultured on phosphate glass specimens for 14 days is presented. In general, cells cultured on all glass surfaces showed a confluent layer after 14 days of culture. However, glass code P50B0 (i.e., containing no boron) appeared to have promoted formation of large nodules of cells which resulted in a nonconfluent layer after 14 days of culture. At initial time points (1, 3 days) glasses containing 1 and 5 mol% boron had greater cell density and attachment sites (lamellipodia and filopodia) compared to glass containing 10 mol% boron oxide. Due to the inherent (cancerous) nature of MG63 cells, large nodules of cells were found at initial time points which resulted in the formation of a dense cell layer at later time points. This observation was consistent for all the glass samples. However, no clusters were spotted at any time points on the TCP control, where the cells were densely packed showing spindle-shaped cells.

4. Discussion

In the absence of any modifier oxides, the structure of PBGs consists of PO_4 groups with many non-bridging oxygens, which explains the low melting temperatures and poor chemical durability of PBGs [7]. For PBGs to be applicable in biomedical applications, the composition of the glasses can be tailored to have suitable dissolution properties. Addition of B_2O_3 to sodium aluminium phosphate glasses was found to increase their T_g with almost complete elimination

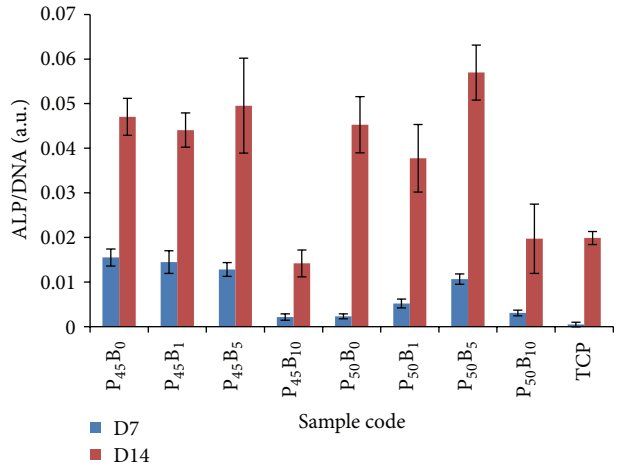

Figure 10: Alkaline phosphate activity of MG63 cultured on PBGs. The data was normalised to DNA concentration. The time points are day 1, 3, 7, and 14. Error bars represent the standard deviation where $n = 6$.

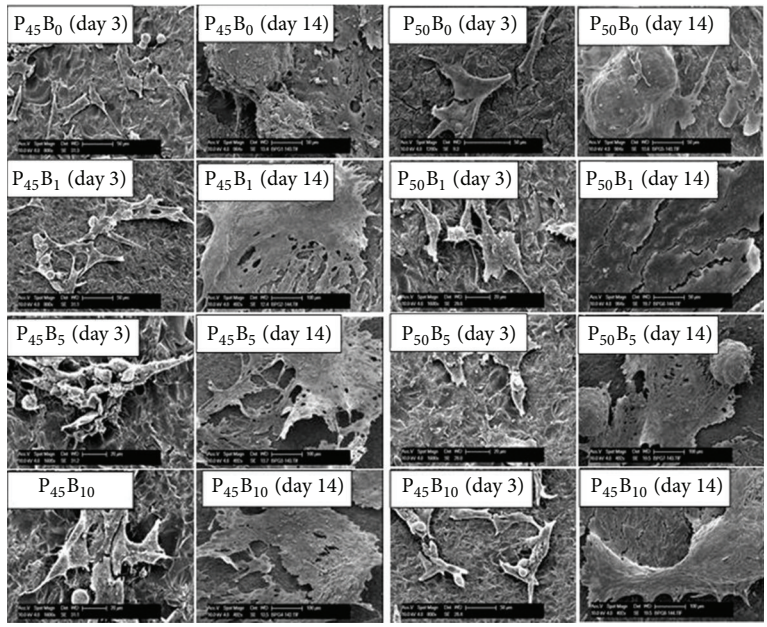

Figure 11: SEM images of MG63 cells cultured on $P_{45}Ca_{16}Mg_{24}Na_{(15-x)}B_x$ (left) and $P_{50}Ca_{16}Mg_{24}Na_{(10-x)}B_x$ (right) after 3 days and 14 days of culture. Micrometer scale bar = 50 μm.

of crystallisation [23]. Similar results with boron addition were also reported for different phosphate glass systems, and their improvement in thermal properties was ascribed to the formation of BO_4 structural units within the phosphate network [16]. 2 mol% boron-modified 45S5 bioglass was found to promote new bone formation more rapidly than standard 45S5 bioglass particles upon implantation into tibial defects in rats [24]. Liang et al. found that scaffolds made with sodium calcium borate glass were converted into hydroxyapatite within 6 days of immersion into K_2PO_4, which supported the attachment and differentiation of human bone marrow derived mesenchymal stem cells and human mesenchymal stem cell derived osteoblasts [25].

All the samples investigated in this study were shown to be amorphous (see Figure 1). It is well known that the physical and thermal properties of glasses are strongly dependent on their structure and composition [11, 15]. As seen from the DSC results, the T_g values increased progressively with the replacement of Na_2O with B_2O_3. Increases of 60°C and 102°C were observed, respectively, for P45 and P50 glasses with 10 mol% B_2O_3 additions, as compared to glasses without B_2O_3. This increase was attributed to the fact that the B-O bond strength is four times higher than that of Na-O bond strength as B^{3+} has a much smaller ionic radius (0.41 Å) compared to Na^+ (1.13 Å). A similar effect on T_g values for replacing Na^+ with Ti^{4+} was observed by Abou Neel et al. where T_g values increased by 155°C with 15 mol% TiO_2 addition due to the smaller ionic radius of Ti^{4+} (0.56 Å) compared to Na^+ [26]. Moreover, Higby et al. reported that

replacement of Na_2O with B_2O_3 caused a decrease in the number of non-bridging oxygens which is also known to increase the T_g [27]. The T_g values were also found to increase as the P_2O_5 content increased from 45 to 50 mol%. Several studies have shown that glasses with 50 mol% P_2O_5 content are dominant in long chains or rings (i.e., Q^2 species), whilst both Q^1 and Q^2 species have been identified for glasses with 45 mol% P_2O_5 [4, 28]. Thus, reducing the P_2O_5 content from 50 to 45 mol% depolymerises the glass network via the introduction of shorter chain Q^1 species which would account for the higher T_g values for P50 glasses as compared to P45 formulations. Ahmed et al. also showed a similar decreasing trend in T_g values with decreasing P_2O_5 content from 50 to 45 mol%; however, with increasing P_2O_5 content from 50 to 55 mol%, the T_g value decreased [28].

An assessment of the thermal stability of the glasses was made in terms of the processing window. Crystallisation temperatures increased with increasing B_2O_3 addition, and the processing window increased (Figure 4). Massera et al. studied the thermal properties of glasses in the system SiO_2-Na_2O-B_2O_3-CaO-MgO-Al_2O_3-P_2O_5 and found that the onset of crystallisation temperature increased as Na_2O was replaced with B_2O_3 [15]. They attributed this change to a reduction in non-bridging oxygens with decreasing amounts of Na_2O [15]. Harada et al. studied glasses in the system BaO-P_2O_5-B_2O_3 and reported that the addition of B_2O_3 suppressed the formation of orthophosphate Q^0 units, which promotes crystallisation. They also suggested that the addition of B_2O_3 suppressed surface crystallisation due to the formation of borate anions and the cross-linked chain structure based on metaphosphate Q^2 tetrahedra [16]. Pemberton et al. and Saranti et al. also suggested that crystallisation occurred from the short chain regions of the glass and that addition of boron could alter the dimensionality of the phosphate network via the formation of long chain Q^2 species rather than Q^0 or Q^1 units [13, 29]. Thus, addition of boron to the phosphate glass network could increase the cross-linking density and also increase the chain length, which in turn would improve the processing window of the glass system as seen from Figure 4.

Initial trials to draw these glass formulations into fibres provided empirical evidence that the larger processing windows obtained due to B_2O_3 incorporation facilitated ease of fibre fabrication for these formulations, as compared to the nonboron containing controls. Continuous fibres of 18–20 micron diameter were successfully drawn from the glass formulation $(P_2O_5)_{45}$-$(CaO)_{16}$-$(Na_2O)_{10}$-$(MgO)_{24}$-$(B_2O_3)_5$ with tensile strength and modulus of 1050 ± 165 MPa and 59.6 ± 5 GPa, respectively.

In addition, through TMA analysis, it was observed that with increasing B_2O_3 content the thermal expansion coefficient decreased, whereas the T_d temperature increased (Figure 5). The thermal expansion coefficient of PBGs is strongly dependent on the cross-link density of the glass network and also on the interaction of the cations with the non-bridging oxygens in the phosphate chain [30]. The cationic field strength is a measure of a cation's effective force for attracting anions and is given by Z/r, where Z is the valency and r is the ionic radius of the cation [31]. Therefore, as B^{3+} has a smaller ionic radius than Na^+ (as discussed above), and the valency is also higher, the field strength of B^{3+} would therefore also be higher than Na^+. This higher field strength of B^{3+} would have a stronger ability to undergo coordination with other groups. The Raman and infrared spectra of the glasses containing B_2O_3 have showed that the addition of B_2O_3 to the phosphate glass structure can form highly cross-linked BPO_4 units which are composed of interconnected BO_4 and PO_4 tetrahedral units [32, 33]. Thus, the higher field strength of B^{3+} compared to Na^+ along with an increase in cross-link density with increasing B_2O_3 content resulted in an increase in T_d and decreased the vibrational movement of the basic structural units, resulting in a decrease in the thermal expansion coefficient values.

The density of the glasses was found to decrease with increasing B_2O_3 content (Figure 6), whereas the molar volume increased (Figure 6). Qiu et al. investigated the density of glasses in the ternary system P_2O_5-B_2O_3-Na_2O and also found that replacement of Na_2O with B_2O_3 decreased the density of their glasses [34]. It was suggested that the density of Na_2O was higher than B_2O_3 in the bulk which could have caused the decrease in density observed with B_2O_3 addition. They also reported that, as B_2O_3 is a network former, the density values may not always reflect the packing density within the glass structure. EL-Hadi et al. studied the density, and molar volume of, a series of sodium borosilicate glasses and found that, by replacing B_2O_3 with Na_2O, the density of the glasses increased, and molar volume decreased [35]. They suggested that addition of Na_2O to the borosilicate glasses increased the amount of non-bridging oxygens and thus reduced the volume which in turn increased the density and decreased molar volume. In this study, a reduction in non-bridging oxygens was expected as Na_2O was replaced with B_2O_3, which correlated well with the existing literature.

A decrease of 55% and 57% in mass loss was observed at 10 mol% B_2O_3 containing P45 and P50 glasses over the time period of 60 days as compared to the glasses with no boron (Figure 7). This decrease in mass loss (%) and dissolution rate with increasing B_2O_3 was attributed to the replacement of P–O–P bonds with P–O–B bonds, which correlated well with an increase in T_g and decrease in thermal expansion coefficient. The chemical bond strength of the diatomic molecule of B–O (808 kJ/mol) is higher than that of P–O (599.1 kJ/mol), suggesting an energetic preference for increased bonding forces inside the glass structure via formation of P–O–B bonds [36]. At higher B_2O_3 content the BO_4 structural unit increased replacing P–O–P bonds with P–O–B bonds which gradually reduced the degradation rate. Shah et al. studied the degradation behaviour of phosphate glasses in the Na_2O-BaO-B_2O_3-P_2O_5 quaternary system and found that the dissolution rate of the glasses decreased with increasing B_2O_3 content [37] which also correlated well with this study.

However, the degradation rate of the glasses was not only affected by the increasing addition of B_2O_3, but the amount of P_2O_5 also affected this dissolution rate. Brauer et al. found that the degradation rate of PBGs reduced by two orders

of magnitude as the P_2O_5 content was reduced from 50 to 45 mol%. Vogel et al. suggested that the reduced degradation rate was due to depolymerisation of the phosphate chain structure from Q^2 to Q^1 species as the Q^2 structures were more susceptible to hydration and subsequent hydrolysis as compared to Q^1 structures [38]. However, it has been reported that the hydration energy for the phosphates decreased in the order of $Q^2 > Q^1 > Q^0$ [39].

The cytocompatibility results showed that incorporation of B_2O_3 (up to 10 mol%) into the glass systems investigated showed no detrimental effect on cell metabolic activity which was comparable to the TCP control (see Figure 9). Cell morphology was also shown to be unaffected for glasses containing B_2O_3 (Figure 11). However, the metabolic activity was significantly lower ($P < 0.001$) for the P50 formulations as compared to the P45 formulations, especially at the initial time points (up to day 7). Hasan et al. [10] reported that the cell metabolic activity and ALP activity of quinternary formulations containing 40–45% P_2O_5 were better than glasses fixed with 50 mol% P_2O_5. They suggested that increased amounts of inorganic phosphate ions released from glass samples containing 50 mol% P_2O_5 could be responsible for the lower cell metabolic and ALP activities as excessive amounts of inorganic phosphate ions are known to be detrimental for cell functions [40]. Ma et al. [41] also reported that the release of excessive inorganic phosphate ions from hydroxyl apatite in cell culture media reduced osteoblast differentiation and mineralisation.

In the current study, ALP activity on all glass samples containing 0–5% B_2O_3 was greater than the TCP control (see Figure 10). A very recent study was carried out to observe the effect of boron (0, 1, 10, 100, and 1000 ng/mL) on osteogenic differentiation of human bone marrow stromal cells (BMSCs), and the results indicated that BMSCs treated with 10 and 100 ng/mL boron presented a higher ALP activity compared to the control [42]. Abou Neel et al. reported that the ALP activity of the phosphate glasses in the system of P_2O_5-CaO-Na_2O was reproducibly enhanced as 3 and 5 mol% TiO_2 were added to the glass system. The authors suggested that this enhancement may be associated with the lower degradation of these compositions which help to maintain the pH at a level favourable for the cellular activity [43]. Ahmed et al. investigated the effect of Fe_2O_3 addition on the CaO-Na_2O-P_2O_5 ternary glass system and found a positive effect of increasing Fe_2O_3 content on cell attachment and differentiation and attributed this towards the increased durability of the glass system [28]. Thus, it could be hypothesised that the improved durability of the glasses with B_2O_3 addition was responsible for the higher ALP activity for the glasses investigated. However, although comparable with the TCP control, the ALP activity of the glasses with 10 mol% B_2O_3 was significantly lower than other glass samples ($P > 0.01$). The lower ALP activity observed for cells cultured on glass samples containing 10% B_2O_3 could possibly be associated with boron ions acting as a stabilising agent for the alkaline phosphatase enzyme [44], which could have cross-linked the enzyme causing lower cleavage of paranitrophenol phosphate (colourless) to paranitriphenol + phosphate (yellow). Zhang et al. [45] investigated porous scaffolds of bioactive borosilicate glasses in the system R_2O-RO-B_2O_3-SiO_2-P_2O_5 with four different contents of borate. It was reported that high cumulative concentrations of boron ions had an inhibitory effect on cell proliferation.

The studies here have shown that boron addition to PBGs has a significant effect on the glass properties via extension of the phosphate chain length and increased processing window. This suggests that continuous manufacture of fibres from glasses with lower phosphate containing content would be possible. This will be investigated in the follow-up study.

5. Conclusions

Eight different phosphate based glass compositions in the system P_2O_5-CaO-Na_2O-MgO-B_2O_3 were produced by replacing the Na_2O with B_2O_3, whilst the P_2O_5 content was fixed to 45 and 50 mol%. The T_g and T_d temperatures increased as Na_2O was replaced with B_2O_3. For both P45 and P50 glasses, the highest T_g was for glasses with 10 mol% B_2O_3. The thermal stability of the glasses was assessed in terms of a processing window and compared to glasses with no boron; the processing window for P45 and P50 glasses increased by 38°C and 36°C with 10 mol% addition of B_2O_3. The thermal expansion coefficient values, density, and dissolution rate decreased with increasing B_2O_3, whereas the molar volume increased. The lowest thermal expansion coefficient (8×10^{-6}°C) and density (2.50×10^3 kg m^{-3}) were observed for glass P50B10. The degradation study revealed a decrease of 55% and 30% in degradation rate for glass codes P45B10 and P50B10 as compared to the controls (P45BO and P50B10). Incorporation of boron into the glass systems investigated showed favourable effects on the cell metabolic activity, proliferation, and morphology. The ALP activity improved for glasses containing 0–5% B_2O_3.However, higher (10%) boron content appeared to have no influence on ALP activity when compared with the TCP control.

Conflict of Interests

The authors do not have any conflict of interest with Birmingham Metal Company (UK), Sigma Aldrich (UK), Norcross (GA, USA), South Bay Technologies (CA, USA), Buehler (Coventry, UK), Fisher Chemicals (UK), Randox (UK), or Falcon, Becton, Dickinson and Company (UK). The companies that provided the materials are listed as is the common practice in journal publications to ensure transparency/reproducibility. None of the authors have any financial or other links to the companies, and as such there is no conflict of interest.

References

[1] L. L. Hench and J. Wilson, "Surface-active biomaterials," *Science*, vol. 226, no. 4675, pp. 630–636, 1984.

[2] L. L. Hench, R. J. Splinter, W. C. Allen, and T. K. Greenlee, "Bonding mechanisms at the interface of ceramic prosthetic

materials," *Journal of Biomedical Materials Research*, vol. 5, no. 6, pp. 117–141, 1971.

[3] L. L. Hench, A. E. Clark, and H. F. Schaake, "Effects of microstructure on the radiation stability of amorphous semiconductors," *Journal of Non-Crystalline Solids*, vol. 8–10, pp. 837–843, 1972.

[4] J. C. Knowles, "Phosphate based glasses for biomedical applications," *Journal of Materials Chemistry*, vol. 13, no. 10, pp. 2395–2401, 2003.

[5] I. Ahmed, M. Lewis, I. Olsen, and J. C. Knowles, "Phosphate glasses for tissue engineering—part 1: processing and characterisation of a ternary-based P_2O_5-CaO-Na_2O glass system," *Biomaterials*, vol. 25, no. 3, pp. 491–499, 2004.

[6] E. A. Abou Neel, D. M. Pickup, S. P. Valappil, R. J. Newport, and J. C. Knowles, "Bioactive functional materials: a perspective on phosphate-based glasses," *Journal of Materials Chemistry*, vol. 19, no. 6, pp. 690–701, 2009.

[7] J. R. van Wazer, *Phosphorus and Its Compounds*, Interscience Publishers Ltd., London, UK, 1958.

[8] S. W. Martin, "Review of the structures of phosphate glasses," *European Journal of Solid State and Inorganic Chemistry*, vol. 28, pp. 163–205, 1991.

[9] I. Ahmed, A. Parsons, A. Jones, G. Walker, C. Scotchford, and C. Rudd, "Cytocompatibility and effect of increasing MgO content in a range of quaternary invert phosphate-based glasses," *Journal of Biomaterials Applications*, vol. 24, no. 6, pp. 555–575, 2010.

[10] M. S. Hasan, I. Ahmed, A. J. Parsons, G. S. Walker, and C. A. Scotchford, "Material characterisation and cytocompatibility assessment of quinternary phosphate glasses," *Journal of Materials Science: Materials in Medicine*, vol. 23, no. 10, pp. 2531–2541, 2012.

[11] D. Carta, D. Qiu, P. Guerry et al., "The effect of composition on the structure of sodium borophosphate glasses," *Journal of Non-Crystalline Solids*, vol. 354, no. 31, pp. 3671–3677, 2008.

[12] D. Qiu, P. Guerry, I. Ahmed et al., "A high-energy X-ray diffraction, 31P and 11B solid-state NMR study of the structure of aged sodium borophosphate glasses," *Materials Chemistry and Physics*, vol. 111, no. 2-3, pp. 455–462, 2008.

[13] A. Saranti, I. Koutselas, and M. A. Karakassides, "Bioactive glasses in the system CaO–B_2O_3–P_2O_5: preparation, structural study and in vitro evaluation," *Journal of Non-Crystalline Solids*, vol. 352, no. 5, pp. 390–398, 2006.

[14] M. Karabulut, B. Yuce, O. Bozdogan, H. Ertap, and G. M. Mammadov, "Effect of boron addition on the structure and properties of iron phosphate glasses," *Journal of Non-Crystalline Solids*, vol. 357, no. 5, pp. 1455–1462, 2011.

[15] J. Massera, C. Claireaux, T. Lehtonen, J. Tuominen, L. Hupa, and M. Hupa, "Control of the thermal properties of slow bioresorbable glasses by boron addition," *Journal of Non-Crystalline Solids*, vol. 357, no. 21, pp. 3623–3630, 2011.

[16] T. Harada, H. In, H. Takebe, and K. Morinaga, "Effect of B_2O_3 addition on the thermal stability of Barium phosphate glasses for optical fiber devices," *Journal of the American Ceramic Society*, vol. 87, no. 3, pp. 408–411, 2004.

[17] L. Koudelka and P. Mošner, "Study of the structure and properties of Pb-Zn borophosphate glasses," *Journal of Non-Crystalline Solids*, vol. 293–295, no. 1, pp. 635–641, 2001.

[18] P. A. Bingham, R. J. Hand, and S. D. Forder, "Doping of iron phosphate glasses with Al_2O_3, SiO_2 or B_2O_3 for improved thermal stability," *Materials Research Bulletin*, vol. 41, no. 9, pp. 1622–1630, 2006.

[19] H. Arstila, E. Vedel, L. Hupa, and M. Hupa, "Factors affecting crystallization of bioactive glasses," *Journal of the European Ceramic Society*, vol. 27, no. 2-3, pp. 1543–1546, 2007.

[20] W. Liang, Y. Tu, H. Zhou, C. Liu, and C. Rüssel, "Borophosphate glass-ceramic scaffolds by a sodium silicate bonding process," *Journal of Non-Crystalline Solids*, vol. 357, no. 3, pp. 958–962, 2011.

[21] F. H. Nielsen, "The emergence of boron as nutritionally important throughout the life cycle," *Nutrition*, vol. 16, no. 7-8, pp. 512–514, 2000.

[22] A. B. Seddon, V. K. Tikhomirov, H. Rowe, and D. Furniss, "Temperature dependence of viscosity of Er^{3+}-doped oxyfluoride glasses and nano-glass-ceramics," *Journal of Materials Science: Materials in Electronics*, vol. 18, no. 1, pp. 145–151, 2007.

[23] I. W. Donald, B. L. Metcalfe, S. K. Fong, and L. A. Gerrard, "The influence of Fe_2O_3 and B_2O_3 additions on the thermal properties, crystallization kinetics and durability of a sodium aluminum phosphate glass," *Journal of Non-Crystalline Solids*, vol. 352, no. 28-29, pp. 2993–3001, 2006.

[24] A. A. Gorustovich, J. M. P. López, M. B. Guglielmotti, and R. L. Cabrini, "Biological performance of boron-modified bioactive glass particles implanted in rat tibia bone marrow," *Biomedical Materials*, vol. 1, no. 3, pp. 100–105, 2006.

[25] W. Liang, M. N. Rahaman, D. E. Day, N. W. Marion, G. C. Riley, and J. J. Mao, "Bioactive borate glass scaffold for bone tissue engineering," *Journal of Non-Crystalline Solids*, vol. 354, no. 15-16, pp. 1690–1696, 2008.

[26] E. A. Abou Neel, W. Chrzanowski, and J. C. Knowles, "Effect of increasing titanium dioxide content on bulk and surface properties of phosphate-based glasses," *Acta Biomaterialia*, vol. 4, no. 3, pp. 523–534, 2008.

[27] P. L. Higby, R. J. Ginther, I. D. Aggarwal, and E. J. Friebele, "Glass formation and thermal properties of low-silica calcium aluminosilicate glasses," *Journal of Non-Crystalline Solids*, vol. 126, no. 3, pp. 209–215, 1990.

[28] I. Ahmed, C. A. Collins, M. P. Lewis, I. Olsen, and J. C. Knowles, "Processing, characterisation and biocompatibility of iron-phosphate glass fibres for tissue engineering," *Biomaterials*, vol. 25, no. 16, pp. 3223–3232, 2004.

[29] J. E. Pemberton, L. Latifzadeh, J. P. Fletcher, and S. H. Risbud, "Raman spectroscopy of calcium phosphate glasses with varying CaO modifier concentrations," *Chemistry of Materials*, vol. 3, no. 1, pp. 195–200, 1991.

[30] P. Y. Shih, S. W. Yung, and T. S. Chin, "Thermal and corrosion behavior of P_2O_5–Na_2O–CuO glasses," *Journal of Non-Crystalline Solids*, vol. 224, no. 2, pp. 143–152, 1998.

[31] Y. Cheng, H. Xiao, and W. Guo, "Influences of La^{3+} and Er^{3+} on structure and properties of Bi_2O_3–B_2O_3 glass," *Ceramics International*, vol. 34, no. 5, pp. 1335–1339, 2008.

[32] N.-J. Kim, S.-H. Im, D.-H. Kim, D.-K. Yoon, and B.-K. Ryu, "Structure and properties of borophosphate glasses," *Electronic Materials Letters*, vol. 6, no. 3, pp. 103–106, 2010.

[33] L. Koudelka and P. Mošner, "Borophosphate glasses of the ZnO–B_2O_3–P_2O_5 system," *Materials Letters*, vol. 42, no. 3, pp. 194–199, 2000.

[34] D. Qiu, P. Guerry, I. Ahmed et al., "A high-energy X-ray diffraction, 31P and 11B solid-state NMR study of the structure of aged sodium borophosphate glasses," *Materials Chemistry and Physics*, vol. 111, no. 2-3, pp. 455–462, 2008.

[35] Z. A. EL-Hadi, H. Farouk, F. A. Khalifa, and F. A. Moustafa, "Molar volume of some sodium silicate and sodium borosilicate glasses," *Communications de la Faculté des Sciences de l'Université d'Ankara. Series B*, vol. 31, pp. 49–57, 1991.

[36] D. R. Lide, *CRC Handbook of Chemistry and Physics: A Ready-Reference Book of Chemical and Physical Data*, CRC Press, 2004.

[37] K. V. Shah, M. Goswami, S. Manikandan, V. K. Shrikhande, and G. P. Kothiyal, "Surface degradation behaviour of sodium borophosphate glass in aqueous media: some studies," *Bulletin of Materials Science*, vol. 32, no. 3, pp. 329–336, 2009.

[38] M. Navarro, C. Aparicio, M. Charles-Harris, M. P. Ginebra, E. Engel, and J. A. Planell, "Development of a biodegradable composite scaffold for bone tissue engineering: physicochemical, topographical, mechanical, degradation, and biological properties," in *Ordered Polymeric Nanostructures at Surfaces*, G. Vancso, Ed., vol. 200, pp. 209–231, Springer, Berlin, Germany, 2006.

[39] D. S. Brauer, N. Karpukhina, R. V. Law, and R. G. Hill, "Effect of TiO_2 addition on structure, solubility and crystallisation of phosphate invert glasses for biomedical applications," *Journal of Non-Crystalline Solids*, vol. 356, no. 44–49, pp. 2626–2633, 2010.

[40] H.-J. Moon, K.-N. Kim, K.-M. Kim et al., "Effect of calcium phosphate glass on bone formation in calvarial defects of Sprague-Dawley rats," *Journal of Materials Science: Materials in Medicine*, vol. 17, no. 9, pp. 807–813, 2006.

[41] S. Ma, Y. Yang, D. L. Carnes et al., "Effects of dissolved calcium and phosphorous on osteoblast responses," *The Journal of Oral Implantology*, vol. 31, no. 2, pp. 61–67, 2005.

[42] X. Ying, S. Cheng, W. Wang et al., "Effect of boron on osteogenic differentiation of human bone marrow stromal cells," *Biological Trace Element Research*, vol. 144, no. 1–3, pp. 306–315, 2011.

[43] E. A. Abou Neel, W. Chrzanowski, S. P. Valappil et al., "Doping of a high calcium oxide metaphosphate glass with titanium dioxide," *Journal of Non-Crystalline Solids*, vol. 355, no. 16-17, pp. 991–1000, 2009.

[44] Y. Kaup, M. Schmid, A. Middleton, and U. Weser, "Borate in mummification salts and bones from Pharaonic Egypt," *Journal of Inorganic Biochemistry*, vol. 94, no. 3, pp. 214–220, 2003.

[45] X. Zhang, H. Fu, X. Liu et al., "In vitro bioactivity and cytocompatibility of porous scaffolds of bioactive borosilicate glasses," *Chinese Science Bulletin*, vol. 54, no. 18, pp. 3181–3186, 2009.